JOURNAL OF APPLIED PHYSICS VOLUME 92, NUMBER 4 15 AUGUST 2002

Optical response of one-dimensional $(Si/SiO_2)_m$ photonic crystals

M. Patrini,[a] M. Galli, M. Belotti, L. C. Andreani, and G. Guizzetti
INFM and Dipartimento di Fisica "A. Volta," Università di Pavia, 27100 Pavia, Italy

G. Pucker, A. Lui, and P. Bellutti
ITC-IRST, 38050 Povo-Trento, Italy

L. Pavesi
INFM and Dipartimento di Fisica, Università di Trento, 38050 Povo-Trento, Italy

(Received 12 March 2002; accepted for publication 20 May 2002)

One-dimensional photonic crystals made of $(Si/SiO_2)_m$ multilayers with $m=2,...8$ have been grown on SiO_2 4-in. wafers by repeated polysilicon low-pressure chemical vapor deposition, oxidation, and wet etching steps. The poly-Si and SiO_2 layers were about 220 and 660 nm thick, respectively, thus realizing $\lambda/4$ distributed Bragg reflectors. Spectroscopic ellipsometry in the 1.4–5 eV range was used to determine the dielectric function of poly-Si and the actual layer thicknesses, as well as to check the structural and compositional homogeneity of the structures. In order to measure the photonic crystal properties, specular reflectance and transmittance measurements were performed from 0.2 to 6 eV at different angles of incidence $\theta \leqslant 50°$ and for transverse electric and transverse magnetic polarizations. The stop-bands characteristic of Bragg reflector multilayers appear up to the fifth order and become more pronounced with increasing m, reaching almost complete rejection for $m=4$ periods. The experimental spectra were fitted by the transfer-matrix method, both versus θ and m. Moreover, the experimental stop bands of the finite multilayers matched the calculated photonic band gaps of an infinite one-dimensional photonic crystal very well. © *2002 American Institute of Physics.* [DOI: 10.1063/1.1492866]

I. INTRODUCTION

Silica on silicon was among the first technologies to be applied to the manufacturing of optical components and, in the 1990s, to expand the capabilities of Si-based optoelectronic integrated circuits. The high dielectric contrast at the Si/SiO_2 interface ($\Delta n \cong 2$) produces a high reflectance at normal incidence, allowing the fabrication of Si/SiO_2-based photonics devices such as: dual vertically integrated waveguides at $\lambda = 1.3\ \mu m$, produced by the separation-by-implanted-oxygen (SIMOX) technique;[1,2] microcavities consisting of Si/SiO_2 distributed Bragg reflectors (DBR) and SiO_2:Er active region, resonant at 980 nm, realized by sputtering;[3] and DBRs grown by a modified SIMOX technique combined with solid-source Si molecular beam epitaxy,[4] which were demonstrated to have high potential for the control of quantum confinement structures. More recently Si/SiO_2 microcavities with Si:Er active layer tuned for 1.54 μm have been fabricated by plasma-enhanced chemical vapor deposition.[5]

In all the above work, Si/SiO_2 stacks with period number m ranging from 2 to 5 were used with the aim of obtaining high reflectance, without systematically studying the optical properties of these structures. For this reason, in this work we present a study of the optical response of $(Si/SiO_2)_m$ multilayers, with m ranging from 2 to 8. These samples were grown by low-pressure chemical vapor deposition (LPCVD) a widely used technique in microelectronics industry, and recently employed to prepare $SiO_2/Si/SiO_2$ quantum wells[6] and Si/SiO_2 superlattices.[7]

Transmittance and reflectance spectroscopies at different incidence angles and polarizations, as well as spectroscopic ellipsometry, are used to optically investigate the samples in the near infrared (NIR) to vacuum ultraviolet (VUV) spectral range. The main goals are: (i) to check the optical quality and uniformity of samples grown by LPCVD: (ii) to verify the correspondence of the measured properties to the designed ones; and (iii) to analyze the optical response of the multilayer structures on the basis of theoretical models, in particular with respect to their behavior as one-dimensional (1D) photonic crystals. These steps are undertaken in view of obtaining three-dimensional photonic crystals by patterning and etching of multilayers; the Si/SiO_2 system is very favorable for this purpose because of the low number of periods required for high reflectance, as well as the excellent technological control of the etching of both materials. A theoretical study of the photonic bands of etched multilayers has recently been performed.[8]

II. GROWTH OF $(SiO_2/Si)_m$ MULTILAYERS

The growth of Si/SiO_2 multilayers was performed in a LPCVD industrial reactor on a 4 in. SiO_2 wafer. The reproducibility of layer deposition with LPCVD is one of the most important parameters in order to obtain good DBRs, since the optical transmittance and reflectance critically depend on the layer thickness and periodicity. The control of the Si layer thickness is quite challenging, while the control of the SiO_2 layers is readily achieved, for example, in complementary metal–oxide–semiconductor technology. Our processing approach[7] is based on the following procedures: (i) using poly-Si deposition conditions, which give reproducible and

[a]Electronic mail: patrini@fisicavolta.unipv.it

 © 2002 American Institute of Physics

Downloaded 25 Sep 2002 to 193.206.67.98. Redistribution subject to AIP license or copyright, see http://ojps.aip.org/japo/japcr.jsp

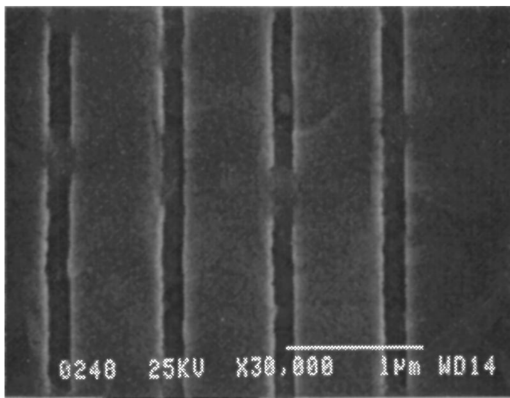

FIG. 1. Scanning electron microscopy image of 8-period Si/SiO_2 distributed Bragg reflector grown by LPCVD.

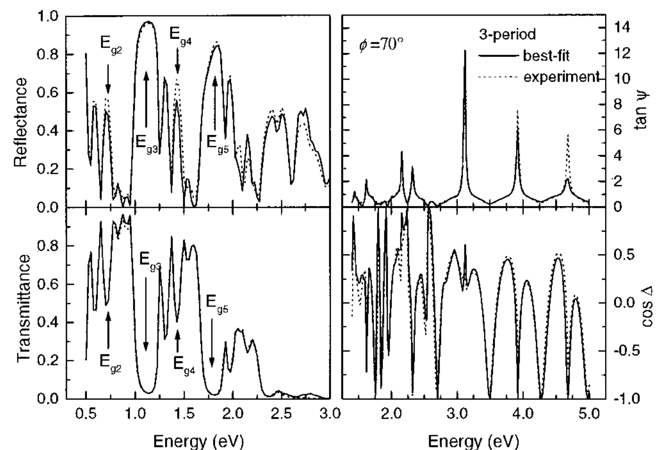

FIG. 2. Reflection (*R*), transmission (*T*), and spectroscopic ellipsometry (SE) experimental spectra of 3-period Si/SiO_2 DBR (dotted lines). The best-fit curves within the full multilayer model are also displayed (solid lines). Arrows mark the photonic band gaps E_{gn} clearly visible in both *R* and *T* spectra.

uniform thin layers, (ii) reduction of these Si layers to the thickness designed by means of an oxidation process, and (iii) deposition of SiO_2 to achieve the designed thickness for the SiO_2 layer. By sequential repetition of the poly-Si deposition, oxidation, and SiO_2 deposition, multilayered structures were obtained. The first step in multilayer growth consists of a poly-Si deposition on an amorphous (a) SiO_2 wafer (double-side polished) at 620 °C and with SiH_4 pressure of 280 mTorr. The layer thickness was 300±10 nm and was estimated with single wavelength ellipsometry at 633 nm by using a HeNe laser. The poly-Si layer was then thinned to about 230 nm by a wet oxidation (in H_2, O_2) at 975 °C. This process resulted in the growth of 140 nm of a-SiO_2. The SiO_2 layer was then further enlarged by deposition of 500 ±15 nm SiO_2 [using tetraethylorthosilicate at 718 °C]. These three steps were repeated to achieve the required number of periods *m*. As the deposition in a LPCVD reactor occurs on both sides of the wafers, the layers from the back side of the wafer were eliminated by a series of wet and dry etching processes. The samples analyzed in this work were $(Si/SiO_2)_m$ multilayers with $m=2$, 3, 4, 6, and 8. The nominal layer thicknesses were 229 and 658 nm for poly-Si and SiO_2 layers, respectively. These values were designed in order to realize λ/4 DBRs, i.e., with the thickness of each layer being inversely proportional to its refractive index. In Fig. 1 a typical scanning electron microscope image of an 8-period sample is shown.

III. EXPERIMENT

Reflectance (*R*) and transmittance (*T*) at normal incidence were measured in the energy range from 0.2 to 3 eV with a Bruker FTIR IFS66 spectrometer, at a spectral resolution of 1 meV; moreover, in the 0.4–6 eV range (NIR-UV) *T* and *R* were measured at different angles of incidence using a Cary 5E automatic spectrophotometer, with a photometric accuracy of ±0.005 and spectral resolution better than 0.5%. An Al mirror, whose absolute reflectivity was directly measured, was used as reference for *R* in the entire spectral range. Using a *V*-*W* accessory the absolute value of *R* at normal incidence was also checked. The spectra from different instruments merge one into the other, within the experimental uncertainty. Polarized measurements at oblique incidence were performed both in transverse electric (TE) and transverse magnetic (TM) polarizations by means of a calcite Glan–Taylor polarizer.

The ellipsometric functions $\tan\psi$ and $\cos\Delta$ [with $\tilde{\rho}=\tan\psi\exp(i\Delta)$, where $\tilde{\rho}=\tilde{r}_p/\tilde{r}_s$ is the complex ratio of the parallel ($\tilde{r}_p$) to the perpendicular ($\tilde{r}_s$) polarization reflection coefficients] were measured between 1.4 and 5 eV by an automatic ellipsometer (Sopra model MOSS ES4G). The system uses a rotating polarizer, an auto-tracking analyzer, a double monochromator and a single-photon-counting photomultiplier detector system. $\tan\psi$ and $\cos\Delta$ (SE) spectra were acquired with a typical standard deviation of less than 0.005, with a mesh of 10 meV, and a spectral resolution of 1 meV, at two angles of incidence ($\theta=75\pm0.05°$ and $70\pm0.05°$) close to the Brewster angle for optimum sensitivity.

In order to test compositional and thickness uniformity, measurements were performed on four different areas of the wafers. The spectra from different points coincide within experimental uncertainty so that the samples can be considered laterally homogeneous.

IV. RESULTS AND MODELING

In Figs. 2 and 3, *R, T*, and SE experimental and fitted spectra of 3- and 6-period DBRs are reported. We note several fringes typical of multilayer interferences. In the *R* and *T* spectra, two major features, maxima in *R* and minima in *T*, are observed for all the samples at 1.14 and at 1.81 eV, respectively, and are labeled E_{g3} and E_{g5}. The labeling has been chosen in agreement with the theory presented in Sec. V. Two additional minor features at 0.67 and 1.39 eV, which are labeled E_{g2} and E_{g4}, are also evident for all the samples. The labeled features correspond to the forbidden gaps (the so-called stop-bands) of the 1D photonic structure. The multilayers have been grown in the λ/4 condition, so that forbidden gaps of odd order (odd index) are wider than forbidden gaps of even order (even index), as expected from the theory in Sec. V. The width of the E_{g3} and E_{g5} gaps are 18% and 9% of the midgap frequency, respectively.

Downloaded 25 Sep 2002 to 193.206.67.98. Redistribution subject to AIP license or copyright, see http://ojps.aip.org/japo/japcr.jsp

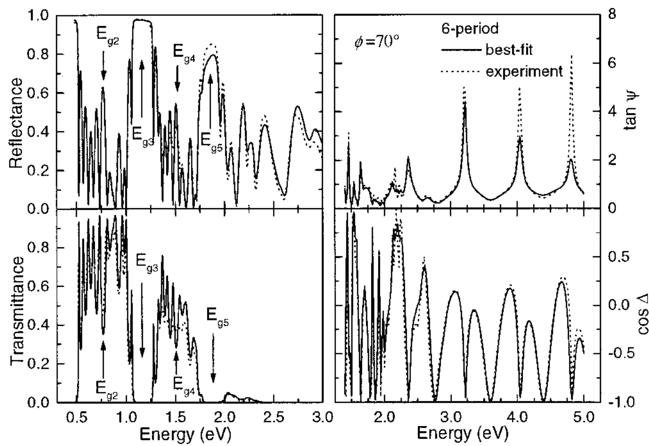

FIG. 3. Reflection (R), transmission (T), and spectroscopic ellipsometry (SE) experimental spectra of 6-period Si/SiO_2 DBR (dotted lines). The best-fits within the full multilayer model are also displayed (solid lines). Arrows mark the photonic band gaps E_{gn} clearly visible in both R and T spectra.

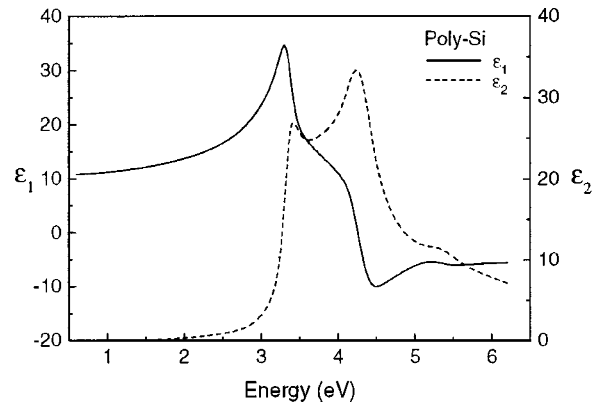

FIG. 4. Real (ε_1) and imaginary (ε_2) part of the complex dielectric function $\tilde{\varepsilon}(\omega)$ of poly-Si layers grown by LPCVD, as derived from ellipsometric measurements in the effective medium approximation.

Absorption from poly-Si becomes relevant at photon energies greater than 1.5 eV, as is evident in the T spectra, and causes the transmitted intensity to reduce to zero for energies greater than 3 eV. By increasing the number of periods m we note three major effects. The first one is the modification of the shape and amplitude of the R and T features. Deeper transmittance minima and reflectance close to unity in the stop-bands indicate an improved rejection ratio both in the even and odd band gaps. Moreover the stop-band edges become sharper for E_{g3} and E_{g5}. Secondly, the appearance of additional interference fringes in the R and T spectra is due to the higher number of periods. The third effect is the increase of absorption at high energies due to the increased overall poly-Si thickness.

The optical response of the samples was calculated in a multilayer model (MLM) with the transfer-matrix method developed by Abèles.[9] The 2×2 complex matrix $\tilde{\mathbf{S}}$, describing light propagation into a multilayer on a substrate, is given by the product

$$\tilde{\mathbf{S}}=\mathbf{I}_{01}\mathbf{L}_1\mathbf{I}_{12}\mathbf{L}_2\mathbf{I}_{21}\ldots\mathbf{L}_{\mathrm{sub}}\mathbf{I}_{\mathrm{sub}0}, \tag{1}$$

where $\mathbf{L}$ and $\mathbf{I}$ are the layer propagation matrix and the interface propagation matrix, respectively, and the labels 0 and sub refer to vacuum and substrate, respectively. The matrix $\mathbf{L}_j$ relative to the jth layer is given by

$$\mathbf{L}_j=\begin{bmatrix} e^{i\tilde{\beta}_j} & 0 \\ 0 & e^{-i\tilde{\beta}_j} \end{bmatrix},$$

with

$$\tilde{\beta}_j=\frac{2\pi d_j\tilde{n}_j}{\lambda}\cos\theta_j, \tag{2}$$

where θ_j is the incidence angle, λ the light wavelength, d_j the thickness, and $\tilde{n}_j$ the complex refractive index of the jth layer. The matrix $\mathbf{I}_{(j-1)j}$ at the interface between $(j-1)$th and jth layer is given by

$$\mathbf{I}_{(j-1)j}=\frac{1}{1+\tilde{r}_{(j-1)j}}\begin{bmatrix} 1 & \tilde{r}_{(j-1)j} \\ \tilde{r}_{(j-1)j} & 1 \end{bmatrix}, \tag{3}$$

where $\tilde{r}_{(j-1)j}$ is the complex Fresnel reflection coefficient at the interface. From the $\tilde{\mathbf{S}}$ matrix elements we can obtain the reflectance $R=|\mathbf{S}_{12}/\mathbf{S}_{11}|^2$ and the transmittance $T=|1/\mathbf{S}_{11}|^2$. All results apply both to TE and TM polarizations, yielding also the complex refraction amplitude ratio $\tilde{\rho}$.

In order to construct the $\mathbf{L}$ and $\mathbf{I}$ matrices it is necessary to know $\tilde{n}$ of both SiO_2 and poly-Si layers. $\tilde{n}$ of amorphous silicon dioxide was measured by SE on a reference sample, made of a 650-nm-thick SiO_2 layer grown on a silicon wafers in the same conditions as the oxide layers in the multilayers. SE measurements give the dielectric functions ε_1 and ε_2 of the SiO_2, thus yielding $\tilde{n}=\sqrt{\tilde{\varepsilon}}=\sqrt{\varepsilon_1+i\varepsilon_2}$ spectra, in good agreement with those reported in literature.[10]

$\tilde{n}$ of poly-Si was obtained using a Bruggeman effective medium approximation (EMA).[11] The poly-Si layer can be assumed as a microscopically heterogeneous material consisting of a random mixture of three separate phases: crystalline silicon, amorphous silicon, and voids.[12,13] In EMA the phases have to be large enough to preserve their individual dielectric functions, but smaller than the wavelength of the probing light. A single poly-Si reference layer grown over a SiO_2 substrate was measured by SE, and the ellipsometric functions $\tan\psi$ and $\cos\Delta$ were fitted by parametrizing its dielectric function with a Bruggeman three-phase mixture. The volume fractions of the separate phases were the free parameters, while the $\tilde{\varepsilon}$ function of each phase was taken from literature.[10] The poly-Si layer resulted from best-fit in a mixture of 89.6% c-Si, 8.3% a-Si, and 2.1% voids. The corresponding ε_1 and ε_2 spectra are shown in Fig. 4.

Finally R, T, and SE spectra were fitted to the full MLM keeping the poly-Si and SiO_2 layer thicknesses as free parameters. The spectra from 0.25 to 6 eV of R and T at normal incidence and of $\tan\psi$ and $\cos\Delta$ at two different incidence angles were fitted simultaneously using the software package by Woollam Inc, based on Levemberg–Marquardt algorithm. The best-fit results are shown in Figs. 2 and 3. Starting from nominal fabrication thicknesses we obtain the following average values: 220 ± 7 nm for the poly-Si layers and 615 ±20 nm for the SiO_2 layers; these values are systematically 5% lower than the nominal ones.

Downloaded 25 Sep 2002 to 193.206.67.98. Redistribution subject to AIP license or copyright, see http://ojps.aip.org/japo/japcr.jsp

V. DISCUSSION

The comparison between best-fit curves, obtained from the MLM and the EMA, and experimental spectra shows a very good agreement. Apart from minor discrepancies in high m multilayers, the fit reproduces all interference structures generated by multiple reflections at the interfaces; this demonstrates that the adopted model is adequate, supporting the MLM assumption of plane homogeneous layers with sharp interfaces.

The results were compared with theoretical calculation of the 1D photonic band dispersion along the axis of the multilayer. Maxwell equations together with the use of Bloch theorem for a 1D periodic structure lead to the following secular equation describing the $\omega(k)$ dispersion:[14]

$$\cos kd = \cos k_1 L_1 \cos k_2 L_2 - \frac{1}{2}\left(\frac{n_1}{n_2} + \frac{n_2}{n_1}\right) \times \sin k_1 L_1 \sin k_2 L_2, \tag{4}$$

where k is the Bloch vector along the multilayer axis, $d = L_1 + L_2$ is the period, and L_j, n_j, $k_j = n_j(\omega/c)$ are thickness, refractive index, and wave vector in the layer j, respectively, with $j = 1,2$ referring to the poly-Si and SiO_2 layers, respectively. The $\omega(k)$ dispersion derived from above equation represents the 1D photonic band dispersion for an infinite multilayer. Note that the frequency dependence of ε in both SiO_2 and poly-Si can be taken into account by simply letting $n_j \rightarrow n_j(\omega)$. Resulting photonic bands are shown in Fig. 5 together with R and T experimental spectra of the 4-period multilayer. We note that the calculated photonic gap positions match very well the T minima and R maxima. According to the choice of designing $\lambda/4$ Bragg reflectors, the odd gaps (E_{g1}, E_{g3}) that lie at Brillouin zone (BZ) edge are larger, while even photonic gaps (E_{g2}, E_{g4}) at the center of the BZ are smaller. The theory shows that, in the case of a frequency-independent ε, these odd gaps should disappear. In the 0.12–0.25 eV energy range, SiO_2 is highly absorbing due to the transverse optical phonon resonance, as is evident in the experimental spectra where T reduces rapidly to zero; this effect has not been taken into account in the calculation of the photonic bands displayed in Fig. 5.

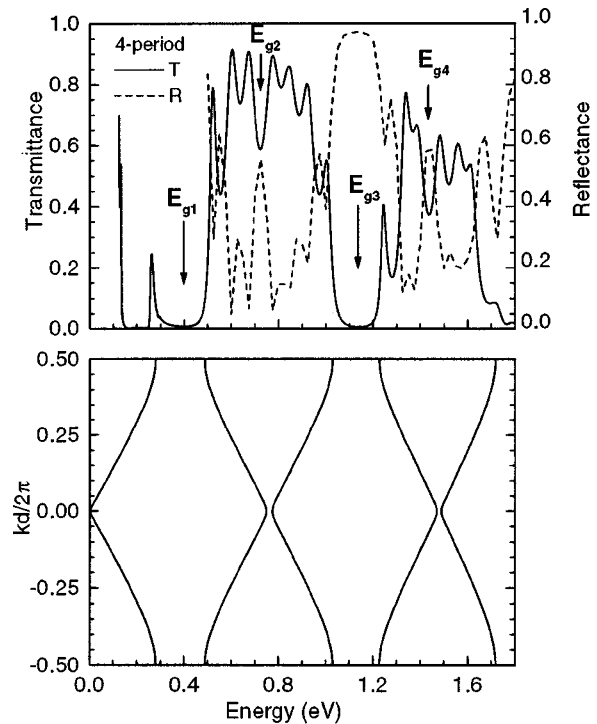

FIG. 5. Photonic band dispersion calculated for an infinite 1D Si/SiO_2 photonic crystal compared to the optical response in reflectance (dotted) and transmittance (solid) of the 4-period DBR sample in the same spectral range. The energies at the center of the photonic gaps are marked by arrows.

While the calculated photonic bands are a property of an infinite multilayer, the T and R spectra are obviously taken on samples with a finite number of periods. This has two consequences. First, the transmittance at the center of each gap decreases exponentially with increasing m, according to the well-known formula $T \propto (n_L/n_H)^{2m}$, where n_L (n_H) represents the low (high) refractive index. Due to the large refractive index contrast between Si and SiO_2, low transmittance values are obtained already with a small number of periods for the odd gaps E_{g1}, E_{g3}, and E_{g5}. Second, the T and R spectra on a sample with m periods display $m-1$ interference oscillations in the frequency window between two gaps: this corresponds to the 1D photonic bands whose wave vector is discretized according to the total multilayer thickness. Thus each transmittance maximum should be viewed as being due to the excitation of a discretized photonic mode. This explains why the sample with $m=4$ periods has three transmission maxima between two gaps (Fig. 5), while the $m=6$ period sample has five transmission maxima (Fig. 3).

The absolute values of T in the photonic gaps have been analyzed as a function of the number of periods m. In Fig. 6, the minima T values in E_{g3} at about 1.14 eV and E_{g5} at about 1.81 eV are reported and compared with theoretical values calculated using the transfer-matrix method. As expected, the efficiency of the DBRs increases with an increasing number of periods. We note that experimental and theoretical T values show very good agreement.

T values in the photonic band gaps have been evaluated versus the incidence angle $\theta \leq 50°$ with both TE and TM light polarization. In Fig. 7 the experimental and calculated T values are shown for the 3-period sample. The two light polarizations have been considered in order to evaluate the symmetry breaking effect on the optical response. T should depend on θ according to the following calculated expressions:[15]

$$T(\theta) = 4\frac{n_s}{n_0}\frac{\cos\theta_s}{\cos\theta}\left(\frac{n_1\cos\theta_1}{n_2\cos\theta_2}\right)^{2m} \quad \text{for TE polarization,} \tag{5a}$$

for TE polarization, and

$$T(\theta) = 4\frac{n_s}{n_0}\frac{\cos\theta}{\cos\theta_s}\left(\frac{n_1\cos\theta_2}{n_2\cos\theta_1}\right)^{2m} \quad \text{for TM polarization,} \tag{5b}$$

where the subscripts 0, 1, 2, and s refer to the vacuum, SiO_2, poly-Si, and substrate, respectively. The experimental values in Fig. 7 correspond to the photonic gaps E_{g3} at ~1.14 eV

Downloaded 25 Sep 2002 to 193.206.67.98. Redistribution subject to AIP license or copyright, see http://ojps.aip.org/japo/japcr.jsp

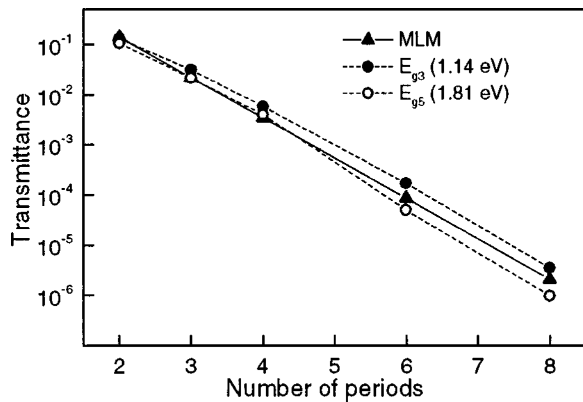

FIG. 6. Transmittance values at the middle of the photonic gaps E_{g3} and E_{g5} (solid and open circles, respectively) in Si/SiO_2 DBRs versus the period number m. T values as calculated by the full multilayer model are also reported (up triangles).

and E_{g5} at ~1.81 eV. For the angular dispersion of the first stop-band the agreement is very good, while for the second one T values are quite different because of the increased absorption of poly-Si layer.

VI. CONCLUSIONS

$(Si/SiO_2)_m$ multilayers with periods m ranging from 2 to 8 were grown by LPCVD, in order to realize $\lambda/4$ DBRs. The optical response of these 1D photonic crystals was measured by reflectance and transmittance from 0.2 to 6 eV at different angles of incidence and polarizations, and by spectroscopic ellipsometry in the 1.4–5 eV photon energy range. The simultaneous fit of R, T, and SE spectra with the multilayer model, using the transfer matrix model and the effective medium approximation, yielded the thickness of the layers and the dielectric function of poly-Si, R and T spectra clearly evidenced the stop-bands of the DBRs up to the fifth order, with the following features:

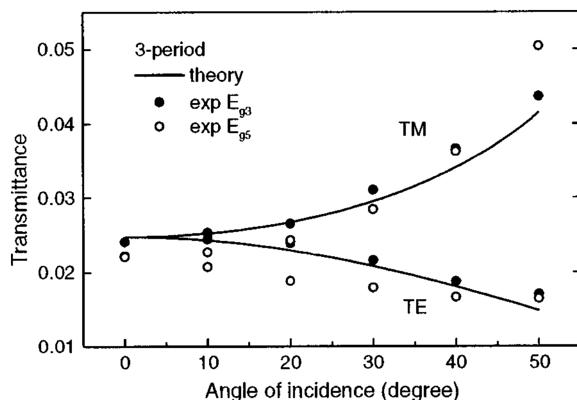

FIG. 7. Transmittance values at the middle of the photonic gaps E_{g3} and E_{g5} (solid and open circles, respectively) in a 3-period Si/SiO_2 DBR versus the angle of incidence and for TE and TM polarizations. Theoretical values for the same sample are also reported (solid lines).

(i) the odd photonic gaps are wider and more sharply defined than even ones, according to the theoretical predictions for a multilayer close to $\lambda/4$ condition;

(ii) the T value at the center of each photonic gap decreases exponentially with increasing m;

(iii) in a m-period sample R and T spectra display $m-1$ interference fringes in the spectral interval between two adjacent gaps: this follows from the 1D photonic bands whose wave vector is discretized according to the finite total thickness of the multilayer;

(iv) for oblique incidence the photonic gaps shift to higher energies; the corresponding T values have a different behavior in TE and TM polarizations;

(v) the experimental values (energy position and width) of the photonic gaps agree very well with those calculated for an infinite 1D photonic crystal.

The experimental results and their overall good agreement with theoretical predictions demonstrate that these $(Si/SiO_2)_m$ structures present good optical quality and should be designed and used as 1D photonic crystals with high refractive index contrast and good rejection rate even for small m values. This opens up possibilities in terms of patterned Si/SiO_2 multilayers in order to realize three-dimensional photonic crystals with a conventional growth technique like LPCVD deposited on Si or SiO_2 substrates. Phase-sensitive optical measurements on the same samples are in progress on a fixed white-light Mach–Zehnder interferometer. The apparatus is used to directly measure the photonic band structure through the phase-shift in the optical response introduced by the lattices.

ACKNOWLEDGMENTS

This work was supported in part by MURST through Cofin 2000 project "One and two-dimensional photonic crystals: growth, theory and optical properties."

[1] F. Namavar, E. Cortesi, R. A. Soref, and P. Sioshansi, Mater. Res. Soc. Symp. Proc. **147**, 235 (1989).
[2] R. A. Soref, E. Cortesi, F. Namavar, and L. Friedman, IEEE Photonics Technol. Lett. **3**, 22 (1991).
[3] E. F. Schubert, N. E. J. Hunt, A. M. Vredenberg, T. D. Harris, J. M. Poate, D. C. Jacobson, Y. H. Wong, and G. J. Zydzik, Appl. Phys. Lett. **63**, 2603 (1993).
[4] Y. Ishikawa, N. Shibata, and S. Fukatsu, Appl. Phys. Lett. **69**, 3881 (1996); Thin Solid Films **321**, 234 (1998).
[5] M. Lipson and L. C. Kimerling, Appl. Phys. Lett. **77**, 1150 (2000).
[6] V. Mulloni, R. Chierchia, C. Mazzoleni, G. Pucker, and L. Pavesi, Philos. Mag. B **80**, 705 (2000).
[7] G. Pucker, P. Bellutti, C. Spinella, K. Gatterer, M. Cazzanelli, and L. Pavesi, J. Appl. Phys. **88**, 6044 (2000).
[8] E. Pavarini and L. C. Andreani, Phys. Rev. E (to be published).
[9] F. Abelès, J. Phys. (France) **11**, 310 (1950).
[10] *Handbook of Optical Constants of Solids*, edited by E. D. Palik (Academic, Orlando, 1985).
[11] J. C. M. Garnett, Philos. Trans. R. Soc. London, Ser. A **203**, 385 (1904); **205**, 237 (1906).
[12] P. Petrik, T. Lohner, M. Fried, L. P. Birò, N. Q. Khành, J. Gyulai, and H. Ryssel, J. Appl. Phys. **87**, 4 (2000).
[13] P. Petrik, M. Friend, T. Lohner, R. Berger, L. P. Birò, J. Gylai, and H. Ryssel, Thin Solid Films **313–314**, 259 (1998).
[14] A. Yariv and P. Yeh, *Optical Waves in Crystals* (Wiley, New York, 1984).
[15] G. Panzarini, L. C. Andreani, A. Armitage, D. Baxter, M. S. Skolnick, V. N. Astratov, J. S. Roberts, A. V. Kavokin, M. R. Vladimirova, and M. A. Kaliteevski, Phys. Rev. B **59**, 5082 (1999).

Downloaded 25 Sep 2002 to 193.206.67.98. Redistribution subject to AIP license or copyright, see http://ojps.aip.org/japo/japcr.jsp